Journal of King Saud University – Science 32 (2020) 3032–3038

Contents lists available at ScienceDirect

Journal of King Saud University – Science

journal homepage: www.sciencedirect.com

Original article

Excellent antimicrobial performance of co-doped magnetite double-layered ferrofluids fabricated from natural sand

Ahmad Taufiq [a,*], Rosy Eko Saputro [a], Defi Yuliantika [a], Sunaryono Sunaryono [a], Markus Diantoro [a], Arif Hidayat [a], Nurul Hidayat [a], Munasir Munasir [b]

[a] Department of Physics, Universitas Negeri Malang, Jl. Semarang No 5, Malang 65145, Indonesia
[b] Department of Physics, Faculty of Mathematics and Natural Sciences, Universitas Negeri Surabaya, Jl. Ketintang, Selatan Surabaya 60231, Indonesia

ARTICLE INFO

Article history:
Received 15 May 2020
Revised 5 August 2020
Accepted 11 August 2020
Available online 18 August 2020

Keywords:
Co-doped magnetite
Ferrofluid
Double-layer
Nanocomposite
Antimicrobial agent

ABSTRACT

The preparation of Co-doped magnetite ferrofluids from natural sand was developed using a double-layer technique. The Co-doped magnetite nanoparticles formed a spinel phase with lattice parameters in the range of 8.355–8.422 Å and tended to agglomerate with the particle sizes of 7–12 nm. The presence of the first and second layers from oleic acid and DMSO was detected by the infrared spectrum as well as the olive oil used as a carrier liquid. The saturation magnetization of the superparamagnetic samples decreased from 24.4 to 4.8 emu/g with decreasing Co^{2+} composition. The particle size and electrostatic forces between the magnetic particles and the microbes played an essential role in inhibiting microbial growth. Interestingly, the increasing Co^{2+} composition enhanced the superior performance of the ferrofluids against *E. coli, S. aureus, B. subtilis,* and *C. albicans*. With additional extensive investigation, we believe that the prepared Co-doped magnetite double-layered ferrofluids from natural sand with superior antimicrobial performance can be new significant antimicrobial agents.

1. Introduction

In the last few years, a serious global problem is an increase in morbidity and mortality due to infectious diseases caused by pathogenic microbes such as viruses, bacteria, and fungi. Such infections cause at least 400 million deaths annually (Fitzpatrick et al., 2019). Even the Coronavirus pandemic has now infected millions of people in the world in a short time, proving that pathogenic microbes are becoming a severe problem that can threaten human life and the economic stability of many countries. In response, experts from various fields continue to develop methods, especially for synthesis, to produce new antimicrobial drugs that are effective and efficient in overcoming pathogenic microbes. However, the issue of increasing multi-drug resistance from pathogenic microbes has not been addressed (Huang et al., 2014), and the majority of antibiotics mostly works by weakening or killing harmful microbes. However, various microbes can develop resistance to certain antibiotics or even induce mutations (Ruddaraju et al., 2020). Furthermore, the increasing number of pathogenic microbes that are resistant to antibiotics produces diseases, otherwise, it leads to severe death (Kadiyala et al., 2018). Therefore, the development of novel approaches to overcome pathogenic microbes, primarily through the combination of antimicrobial drugs with magnetic nanoparticles, is important. One of the most central reasons for developing novel approaches in fraying infectious diseases of pathogenic microbes is to improve the delivery of antimicrobial materials so as to significantly decrease the minimal inhibition concentrations of the drug used independently (Liakos et al., 2014).

Currently, treatments of pathogenic microbes, particularly metal oxide-based nanomaterials, have been developed by researchers in various fields, given the high specific surface area of nanomaterials that maximize interaction with the microbial membrane (Shuai et al., 2019). Theoretically, metal oxides are believed to inhibit the growth of bacteria by producing oxidative stress and reactive oxygen species (ROS) (Saravanan et al., 2018). Furthermore, metal oxides are able to eradicate microbes effectively, given their low toxicity, stability, and higher selectivity when compared with other materials, especially organic materials

* Corresponding author.
E-mail address: ahmad.taufiq.fmipa@um.ac.id (A. Taufiq).
Peer review under responsibility of King Saud University.

Production and hosting by Elsevier

https://doi.org/10.1016/j.jksus.2020.08.009
1018-3647/

(Stankic et al., 2016). Magnetite nanoparticles are potential nanomaterials to be developed as microbial agents given their attributes of biodegradation, biocompatibility, and acceptability for human consumption. Magnetite nanoparticles also have other superior advantages, such as being environmentally friendly, easily synthesized, non-toxic, possessing a large surface area, and having strong magnetic properties (Mozaffari et al., 2015). However, magnetite nanoparticles easily agglomerate when the particle size gets smaller, thus disrupting the application's performance as antimicrobial agents. Furthermore, for biomedical applications, the magnetite nanoparticle surface needs to be modified for easier suspension in water with high stability to resist the effects of protein and salt in the physiological environment (Huang et al., 2014). Therefore, for antimicrobial applications, the development of magnetite nanoparticles into ferrofluids with high stability that is easily soluble in water is believed as the most effective method when compared to bulk, powder, or even thin films antimicrobial activities. One of the most important factors for the successful application of magnetic nanoparticles is a surface modification by organic/inorganic compounds. Unfortunately, the conventional synthesis of magnetite ferrofluids based on a single layer is less effective as the synthesis time tends to produce less stable ferrofluids. Kurimský et al. reported that the single-layered ferrofluids have unstable performance due to the separation phase of magnetic fillers and carrier liquid (Kurimský et al., 2018), which affect their performance applications because the magnetic fillers are not dispersed optimally. Meanwhile, the current study showed that double-layered ferrofluids provide high stability performance even though stored for a relatively long time (Saputro et al., 2020). Therefore, we developed a magnetite ferrofluid synthesis method with a double-layer-based surfactant technique using a carrier liquid of olive oil in which the magnetite ferrofluids are water-soluble.

Magnetite nanoparticles exhibit unique superparamagnetic performance and are easily controlled and recycled by external magnetic fields, which are advantages of antimicrobial applications (Huang et al., 2014). Furthermore, magnetite nanoparticles also have advantages because they are biocompatible and do not require UV light in eradicating microbes, and it is also easily separated using an external magnetic field after being used as an antimicrobial agent (Groiss et al., 2017; Thakur et al., 2019). Therefore, it is important to develop antimicrobial agents based on magnetite nanoparticles. However, magnetite nanoparticles are less chemically stable because of rapid oxidation by oxygen in the air (Asab et al., 2020). Therefore, the doping process into magnetite by substituting Fe ions with other transition metal ions that have better chemical stability is a powerful approach. Conversely, the increase in the chemical stability of magnetite nanoparticles is also very significant and it should be embraced to enhance the antimicrobial performance. Co may address the low chemical stability of magnetite because it has high chemical stability in various environmental conditions and is one of the best dopant candidates. Klein and co-workers proved that Co-doped magnetite is more stable than magnetite in the air (Klein et al., 2018). Previous research shows that Co-doped magnetite has a much greater magnetocrystalline anisotropy compared to magnetite, and it has high magnetic hysteresis, which is very beneficial for biomedical applications (Dönmez et al., 2019). Furthermore, for the benefit of inexpensive and environmentally-friendly, large-scale antimicrobial applications, the synthesis of ferrofluid double layers in this work was also developed by exploring natural iron sand as a primary source for the precursors.

2. Materials and methods

2.1. Preparation of Co-doped magnetite double-layered ferrofluids

The natural iron sand was employed as the primary source to produce $FeCl_2/FeCl_3$. $CoCl_2$, $AgNO_3$, NH_4OH, NaOH, HCl, PVP, $NaBH_4$, oleic acid, and DMSO were purchased from Merck, and olive oil was purchased from Borges. 20 g of the Fe_3O_4 powders extracted from natural sand was reacted with 58 mL of HCl for 20 min to obtain $FeCl_2/FeCl_3$ solution. 20 mL of the solution was then reacted with $CoCl_2$ 60 min. The mass compositions of the $CoCl_2$ were maintained for 0, 1.12, 2.23, 3.35, 4.45, and 5.55 g and coded as samples

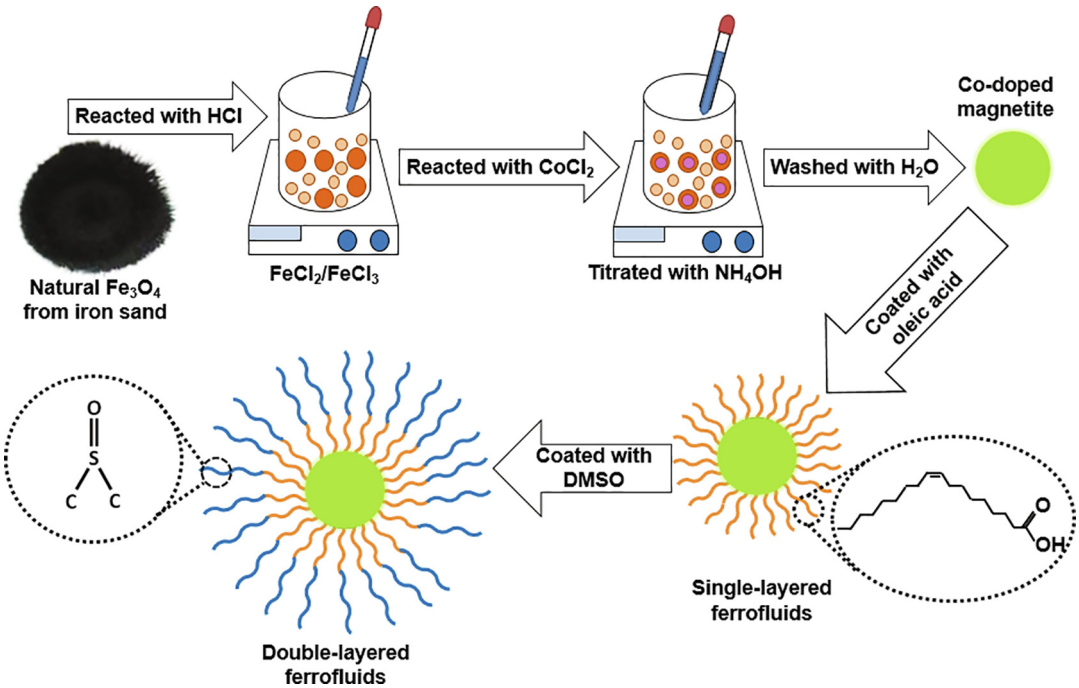

Fig. 1. Illustration of the formation of the Co-doped magnetite double-layered ferrofluids.

S1, S2, S3, S4, S5, and S6, respectively. The final product was titrated with 29 mL of NH_4OH for 30 min and continued by washing and filtering processes to obtain the black precipitated. The black precipitate was mixed with 50 mL of H_2O and sonicated for 10 min and followed by a titration process using NaOH for 30 min until reaching a pH of 11 to obtain a precipitate. The precipitate was covered by 2.5 mL of oleic acid as the first layer. Next, 2.5 mL of DMSO as the second layer was employed by stirring for 60 min to cover the first layer completely. Finally, the final product was dispersed in 10 mL of olive oil as a carrier liquid to obtain the Co-doped magnetite double-layered ferrofluids. The illustration of the formation of ferrofluids is depicted in Fig. 1.

2.2. Characterizations

The synthesized samples were characterized using an X-ray diffractometer (PANalytical X'Pert Pro, Cu-Kα 1.540 Å) and a scanning electron microscope (FEI Inspect-S50) to investigate their lattice parameters, particle size, and morphology. A Fourier transform infrared (FTIR) spectrophotometer (Shimadzu, IRPrestige-21) was employed to evaluate the functional groups of the constituent compound of the ferrofluids. A vibrating sample magnetometer (Oxford VSM1.2H) was employed to investigate the magnetic properties of the samples. All characterizations were conducted at ambient temperature.

The antibacterial activity of the Co-doped magnetite double-layered ferrofluids was evaluated using the agar diffusion method. In this study, chloramphenicol was used as a positive control, and alcohol was used as a negative control. Agar nutrient (NA) was dissolved in distilled water followed by a sterilization process in an autoclave at 150 °C, and thereafter, it was cooled at a temperature of 45 °C and poured in a sterilized petri dish. *S. aureus* and *B. subtilis* colonies were prepared as gram-positive bacteria and *E. coli* bacteria as negative bacteria. Each colony was put in a nutrient broth (NB) to be cultured in a liquid medium for 18 h. In the next stage, all mediums and bacterial cultures were placed in laminar airflow and continued with the inoculation process. The medium containing the sample was put in an incubator at 37 °C for 18 h to obtain the inhibition zone diameter. In this work, three replications were conducted for the experiment.

The antifungal activity of the Co-doped magnetite double-layered ferrofluids was also evaluated using the agar diffusion method. In this work, ketoconazole was used as a positive control, and alcohol was used as a negative control. The antifungal activity test was initiated by dissolving sabouraud dextrose agar (SDA) in distilled water at 200 °C. The SDA medium was sterilized in an autoclave at 150 °C, and thereafter, it was cooled at 45 °C to be poured in a sterilized petri dish. *C. albicans* colonies were prepared and put in NB to be cultured in a liquid medium for 24 h. All mediums and fungal cultures were placed in laminar airflow and continued with the inoculation. Three replications were conducted for the experiment. The inhibition zone diameter of the samples was obtained after maintaining medium containing the sample in an incubator at 37 °C for 18 h.

3. Results and discussions

The XRD patterns of the Co-doped magnetite nanoparticles are depicted in Fig. 2. The XRD data represented by *circles* were fitted well by the calculation model represented by the *solid lines*. Qualitatively, the XRD pattern of each sample had a similar pattern, except for its broadening and peak position. The higher Co^{2+} composition tended to broaden the full width at half maximum, which corresponds to the decreasing particle size from 11.8 to 6.6 nm. The particle size of the samples was also supported by scanning

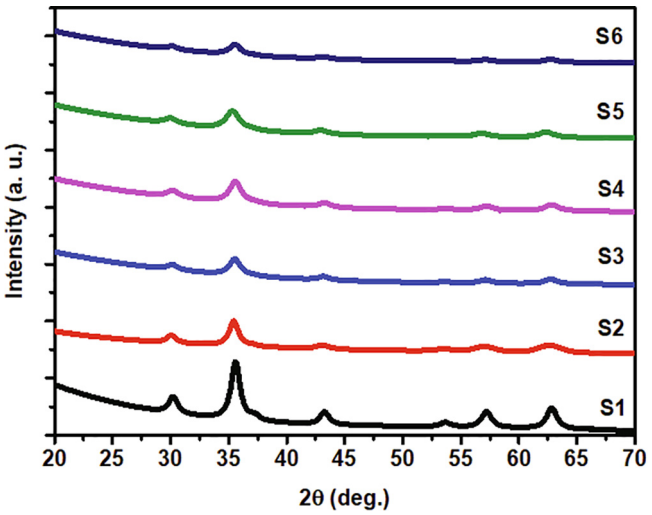

Fig. 2. X-ray diffraction patterns of the Co-doped magnetite nanoparticles.

electron microscopy images, as presented in Fig. 3. Based on the images, the magnetic nanoparticles tend to agglomerate. The agglomeration of the Co-doped Fe_3O_4 nanoparticles was attributed to the van der Waals force between magnetic particles producing the clusters of primary particles (Sunaryono et al., 2016), preventing the formation of a single magnetic domain of the magnetic nanoparticles. The particle sizes of the samples are likely to be stable in the range of 39.9–42.6 nm. These results were higher than those of obtained from X-ray diffraction data since the magnetic nanoparticles agglomerated. The agglomeration of the magnetic nanoparticles in this work was in line with the pDA/PEI/Co^{2+} ternary coated membrane, as reported by Zhang et al. (Zhang et al., 2020b). Interestingly, the presence of Co^{2+} in the magnetite did not produce a new peak, which indicates that Co^{2+} successfully replaced Fe^{3+} (Yang et al., 2016). Moreover, the higher Co^{2+} composition tended to shift the diffraction peak to a lower position, indicating the expansion of the lattice parameters from 8.355 to 8.422 Å in the cubic spinel structure. According to Bragg's law, the lattice parameters expanded because the Co^{2+} has a larger ionic radius (74 pm) than Fe^{3+} (64 pm) (Xiong et al., 2020). As a result, the crystal volume also expanded from 583.2 to 597.4 $Å^3$. Joshi and co-workers successfully synthesized cobalt ferrite nanoparticles with a particle size of approximately 15 nm (Joshi et al., 2016). Swatsitang et al. further produced cobalt ferrite nanoparticles with a particle size of 80–100 nm by varying temperatures (Swatsitang et al., 2016). Therefore, the synthesized Co-doped magnetite nanoparticles prepared from natural sand are smaller than those of the synthesized samples from commercial precursors.

The fitting analysis using the Langevin function (Eq. (1)) was employed, and its results are shown in Fig. 4. Visually, the magnetization curves of all samples had a similar pattern, except for their saturation magnetization value. The curves indicate that the samples form a superparamagnetic character because the remanent magnetization was close to zero (Navgare et al., 2020).

$$M = M_s\left(\coth\left(\frac{\mu H}{k_B T}\right) - \left(\frac{k_B T}{\mu H}\right)\right) \quad (1)$$

Where M, Ms, μ, H, k_B, and T are the magnetization, saturation magnetization, magnetic moment, magnetic field, Boltzmann constant, and temperature, respectively (Rezaei et al., 2018). Based on the fitting analysis, the Ms and magnetic susceptibility (χ) decreased with increasing Co^{2+} composition with the respective values from 24.4 to 4.8 emu/g and from 3.1 to 1.6. In this regard, Daffé et al. explained

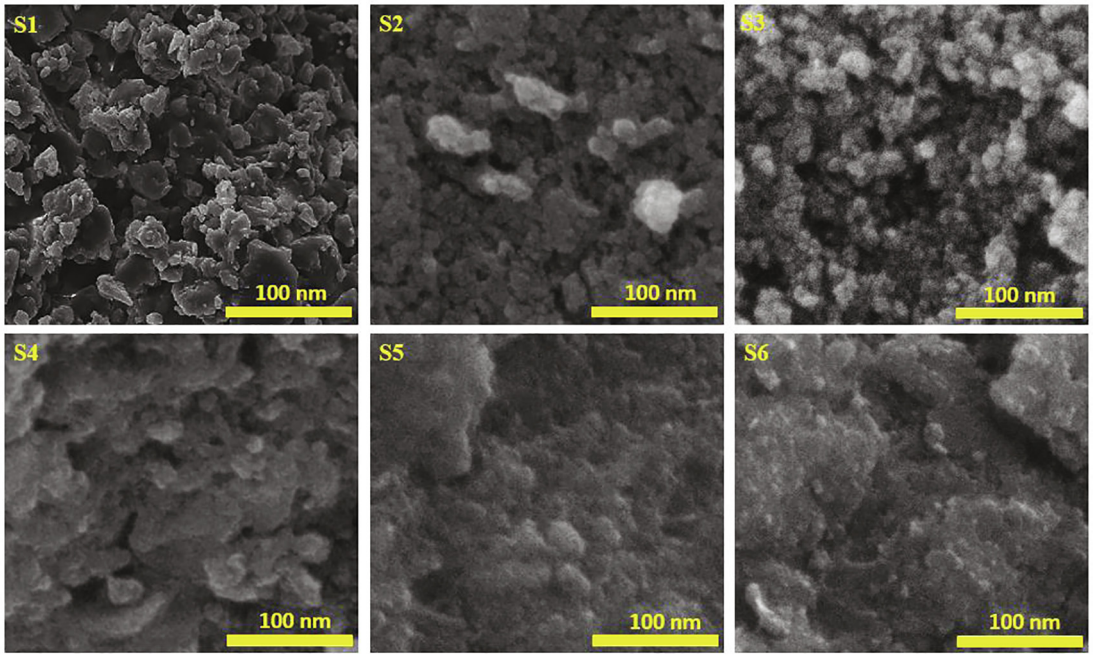

Fig. 3. Scanning electron microscopy images of the Co-doped magnetite nanoparticles.

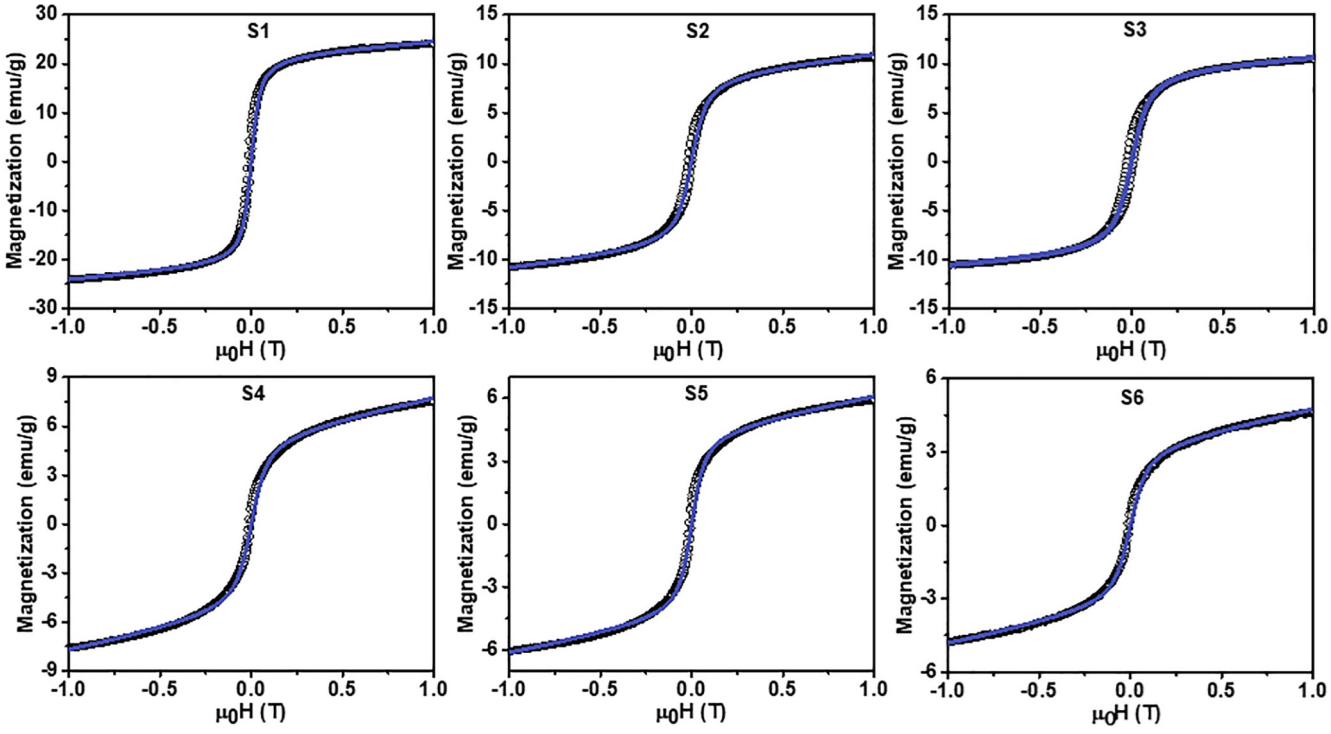

Fig. 4. Fitted magnetization curves of the Co-doped magnetite nanoparticles. The *black circles* and *blue solid lines* represent the respective experimental data and fitting model.

that the physical reason that contributed to such declining values is the presence of the surface disorder and cationic distribution modification owing to the cobalt substitution (Daffé et al., 2018). The magnetic moment of Co^{2+} which is lower than that of Fe^{3+} decreasing *Ms* of the Co-doped magnetic nanoparticles (Purnama et al., 2019).

The functional group of the ferrofluids was investigated to claim the presence of ferrofluid components, as shown in Fig. 5. The first ferrofluid component detected was functional groups of metal oxides (M-O) originating from Fe—O and Co—O. In this work, the presence of M-O was detected at 459 cm^{-1} for the stretching mode at the octahedral position (Husain et al., 2019) and 704 cm^{-1} at the tetrahedral position. Based on the previous work, the stretching mode at the tetrahedral position was in the range of 560 to 580 cm^{-1} (Lei et al., 2017). The displacement was predicted as the effect of the Co^{2+} ions that replaced the Fe^{3+} ions. Furthermore, the decrease in particle size enhanced the forces on the surface of nanoparticles so that the absorption band of FTIR spectrum shifted

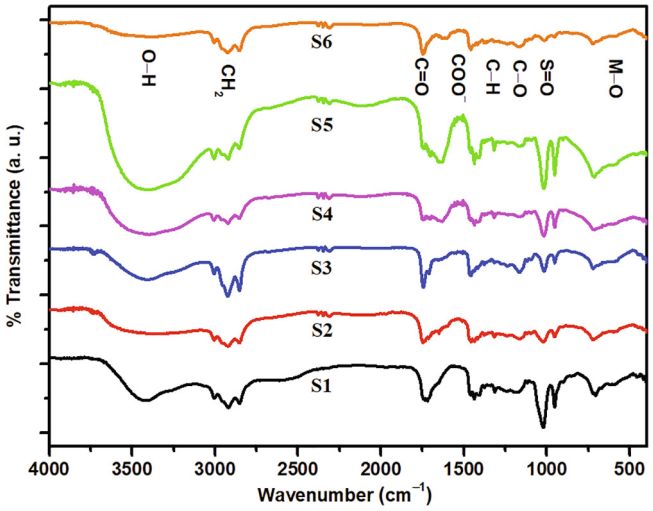

Fig. 5. Infrared spectrum of the Co-doped magnetite double-layered ferrofluids.

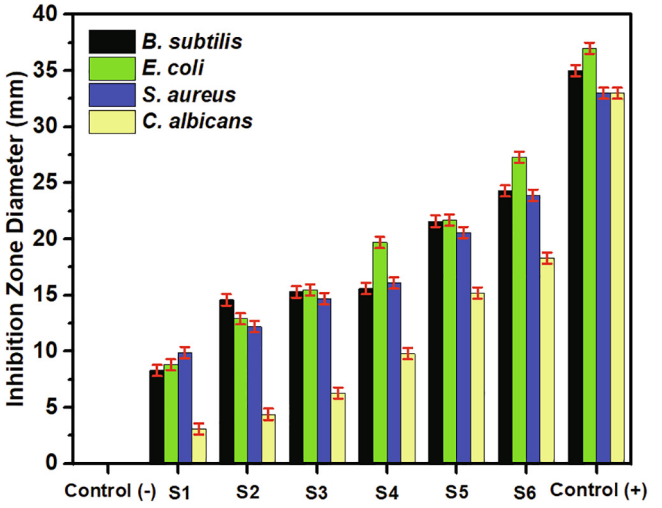

Fig. 6. Inhibition zone diameter of the Co-doped magnetite double-layered ferrofluids. Three replications were maintained for the experiment.

to a higher wavenumber known as the blue shift phenomenon (Jafari et al., 2015). The functional group of oleic acid as the first layer was observed at 1315 and 1377 cm^{-1}, which represented the C=C from oleic acid (Taufiq et al., 2018). Meanwhile, the stretching band that represented the carboxyl group (COO^-) was observed at 1456 cm^{-1} (Marinca et al., 2016). The CH_2 groups and O—H were observed at the respective wavenumbers of 2854–2922 cm^{-1} (Raees et al., 2020) and 3425 cm^{-1} (Zafar et al., 2020). Interestingly, the broadening O—H bond indicated the presence of hydroxyl functional groups which are strongly contributed by surfactants. Furthermore, it was observed that the intensity of O—H functional group fluctuated and tended to have a blue shift phenomenon, indicating the presence of the coupling of dispersants on the surface of ferrofluids. In line with this study, Zhang and co-workers showed that the intensity of O—H functional group decreased by the presence of coupling on the surface of materials (Zhang et al., 2020a). Moreover, the stretching band of DMSO as the second layer was represented by the S=O identified at 954 and 1018 cm^{-1} (Oh et al., 2017). Finally, olive oil as the carrier liquid was observed from the stretching bands of C—H that represented conjugation bond at 1094 cm^{-1}, ester (CO) at 1165 and 1236 cm^{-1} (Mosafer et al., 2017), and carbonyl ester (C=O) at 1655 and 1746 cm^{-1} (Tena et al., 2017). The main bond of the olive oil was the unsaturated bond detected at 3007 cm^{-1} (Taufiq et al., 2017). Therefore, the selection of the olive oil as carrier liquid was appropriate to produce a stable ferrofluid using oleic acid and DMSO as the first and second layers.

The antimicrobial performance of the ferrofluids was represented by the inhibition zone diameter, as shown in Fig. 6. The increasing Co^{2+} composition increased the inhibition zone diameter of the ferrofluids. The increased ability of ferrofluids to inhibit the growth of microbes along with the increased Co^{2+} composition was attributed to the decrease in the size of magnetic particles. Theoretically, by decreasing the particle size, the surface area of the particles surrounding the cell wall gets larger, thus accelerating the damage of the microbial cells (Choi et al., 2019). The small magnetic nanoparticles easily penetrate the cell membrane and react with intracellular oxygen to disrupt the generation of oxidative stress (Nehra et al., 2018). The presence of Co^{2+} can inhibit the oxidation so that the ROS could play an essential role in killing microbial maximally. When the ferrofluids attach to the membrane of the microorganism, it increases the lag phase of the bacterial growth period, prolongs the reproduction time of the microorganism, and increases cell division in the microbial cell (Ashour et al., 2018). Furthermore, the increasing antimicrobial performance of the ferrofluids was also attributed to the free radicals of the superoxide and hydrogen peroxide that was produced on the surface of the materials (Maksoud et al., 2018). Such free radicals penetrate the cell wall of the microbe and produce cell damage quickly.

The surface modification of the Co-doped double-layered ferrofluids also contributed to the inhibition of microbial growth. Theoretically, magnetic nanoparticles in ferrofluids covered by positive charges increased interactions with negatively-charged microbes and produced attractive electrostatic forces between the particle magnetic and microbes (Taufiq et al., 2020), generating more effective in inhibiting the microbial growth. In general, the ferrofluids exhibited more inhibition of *E. coli* than *S. aureus* and *B. subtilis*, which proves that the electrostatic force plays an essential role in inhibiting bacterial growth (Li et al., 2019). The electrostatic attraction between the positively-charged magnetic nanoparticles with negatively-charged Gram-negative bacteria also contributed to the inhibition of bacterial growth. Interestingly, although *E. coli* and *S. aureus* are both negatively charged, the bacterial inhibition performance of the ferrofluids against *E. coli* was superior because *E. coli* has a more negative and less soft surface than *S. aureus* (Sonohara et al., 1995). Therefore, the electrostatic attraction is greater, which ultimately makes it easier for magnetic nanoparticles to penetrate deeper into the bacterial cell wall. Thus, the antimicrobial performance of the Co-doped double-layered ferrofluids did not differ significantly from the antimicrobial performance of each microbial control.

Antimicrobial performance of ferrofluids produced in this research was also supported by the presence of double surfactants, which have good antimicrobial performance. The first surfactant in the form of oleic acid proved effective as an antimicrobial agent. Yoon and colleagues showed that oleic acid aggregates around microbial cell groups and interacts with microbial membranes, which results in malfunction of microbes (Yoon et al., 2018). While in another report, Chen *et al.* identified the effectiveness of the antimicrobial activity of oleic acid against skin infections by *S. aureus* bacteria. They show that oleic acid has an excellent performance so that it can be projected as an antimicrobial agent in the future (Chen et al., 2011). The second surfactant is DMSO which also has a high potential as an antimicrobial agent shown by Ansel and co-workers through exploring the effect of the DMSO composition on its antimicrobial performance. They found that, as the DMSO composition increased, the performance in inhibiting the reproduction of *E. coli*, *P. aeruginosa*, and *B. megaterium* also

increased (Ansel et al., 1969). Furthermore, in another report, it is mentioned that pure DMSO has a potential that is reliable and commonly used as a solvent for antibiotic ingredients (Kirkwood et al., 2018). In double-layered ferrofluids, the control composition of each surfactant plays an essential role in its antimicrobial performance. The composition of the first and second surfactants in the ferrofluid system is not permitted to exceed the composition of the dispersant or carrier liquid to maintain the optimal antimicrobial performance. If the surfactant composition exceeds the composition of the dispersant or carrier liquid in the double-layered ferrofluids, then the surfactant, which acts as a coating for magnetic nanoparticles as fillers, will overlap with the dispersant (Saputro et al., 2020).

4. Conclusions

Co-doped magnetite double-layered ferrofluids were successfully prepared from natural iron sand. The lattice parameters of the Co-doped magnetite nanoparticles enhanced with increasing Co^{2+} from 8.355 to 8.422 Å while their particle size was 7–12 nm. The presence of oleic acid and DMSO as the first and second layers, and olive oil as the carrier liquid, were observed by infrared spectroscopy. The saturation magnetization of the samples decreased with decreasing Co^{2+} from 24.4 to 4.8 emu/g. Fascinatingly, the increasing Co^{2+} composition played an essential role in enhancing the antibacterial and antifungal activities of the Co-doped magnetite ferrofluids.

Declaration of Competing Interest

The authors declare that they have no known competing financial interests or personal relationships that could have appeared to influence the work reported in this paper..

Acknowledgment

This work was partially supported by the research grant from Universitas Negeri Malang under the research expertise group scheme with contract number: 4.3.312/UN32.14.1/LT/2020 for AT.

References

Ansel, H.C., Norred, W.P., Roth, I.L., 1969. Antimicrobial activity of dimethyl sulfoxide against *Escherichia coli*, *Pseudomonas aeruginosa*, and *Bacillus megaterium*. J. Pharm. Sci. 58, 836–839. https://doi.org/10.1002/jps.2600580708.

Asab, G., Zereffa, E.A., Abdo Seghne, T., 2020. Synthesis of silica-coated Fe_3O_4 nanoparticles by microemulsion method: characterization and evaluation of antimicrobial activity. Int. J. Biomater. 2020, 1–11. https://doi.org/10.1155/2020/4783612.

Ashour, A.H., El-Batal, A.I., Maksoud, M.A., El-Sayyad, G.S., Labib, S., Abdeltwab, E., El-Okr, M.M., 2018. Antimicrobial activity of metal-substituted cobalt ferrite nanoparticles synthesized by sol–gel technique. Particuology 40, 141–151. https://doi.org/10.1016/j.partic.2017.12.001.

Chen, C.-H., Wang, Y., Nakatsuji, T., Liu, Y.-T., Zouboulis, C.C., Gallo, R.L., Zhang, L., Hsieh, M.-F., Huang, C.-M., 2011. An innate bactericidal oleic acid effective against skin infection of methicillin-resistant *Staphylococcus aureus*: a therapy concordant with evolutionary medicine. J. Microbiol. Biotechnol. 21, 391–399.

Choi, Y.B., Son, J.H., Bae, D.S., 2019. Fabrication and characterization of Cu doped CeO_2 by hydrothermal process for antimicrobial activity. Defect Diffus. Forum 391, 114–119. https://doi.org/10.4028/www.scientific.net/DDF.391.114.

Daffé, N., Choueikani, F., Neveu, S., Arrio, M.-A., Juhin, A., Ohresser, P., Dupuis, V., Sainctavit, P., 2018. Magnetic anisotropies and cationic distribution in $CoFe_2O_4$ nanoparticles prepared by co-precipitation route: Influence of particle size and stoichiometry. J. Magn. Magn. Mater. 460, 243–252. https://doi.org/10.1016/j.jmmm.2018.03.041.

Dönmez, Ç.E.D., Manna, P.K., Nickel, R., Aktürk, S., van Lierop, J., 2019. Comparative heating efficiency of cobalt-, manganese-, and nickel-ferrite nanoparticles for a hyperthermia agent in biomedicines. ACS Appl. Mater. Interfaces 11, 6858–6866. https://doi.org/10.1021/acsami.8b22600.

Fitzpatrick, M.C., Bauch, C.T., Townsend, J.P., Galvani, A.P., 2019. Modelling microbial infection to address global health challenges. Nat. Microbiol. 4, 1612–1619. https://doi.org/10.1038/s41564-019-0565-8.

Groiss, S., Selvaraj, R., Varadavenkatesan, T., Vinayagam, R., 2017. Structural characterization, antibacterial and catalytic effect of iron oxide nanoparticles synthesised using the leaf extract of *Cynometra ramiflora*. J. Mol. Struct. 1128, 572–578. https://doi.org/10.1016/j.molstruc.2016.09.031.

Huang, K.-S., Shieh, D.-B., Yeh, C.-S., Wu, P.-C., Cheng, F.-Y., 2014. Antimicrobial applications of water-dispersible magnetic nanoparticles in biomedicine. CMC 21, 3312–3322. https://doi.org/10.2174/0929867321666140304101752.

Husain, S., Irfansyah, M., Haryanti, N.H., Suryajaya, S., Arjo, S., Maddu, A., 2019. Synthesis and characterization of Fe_3O_4 magnetic nanoparticles from iron ore 012021. In: Journal of Physics: Conference Series. IOP Publishing. https://doi.org/10.1088/1742-6596/1242/1/012021.

Jafari, A., Shayesteh, S.F., Salouti, M., Boustani, K., 2015. Effect of annealing temperature on magnetic phase transition in Fe_3O_4 nanoparticles. J. Magn. Magn. Mater. 379, 305–312. https://doi.org/10.1016/j.jmmm.2014.12.050.

Joshi, S., Kamble, V.B., Kumar, M., Umarji, A.M., Srivastava, G., 2016. Nickel substitution induced effects on gas sensing properties of cobalt ferrite nanoparticles. J. Alloys Compd. 654, 460–466. https://doi.org/10.1016/j.jallcom.2015.09.119.

Kadiyala, U., Turali-Emre, E.S., Bahng, J.H., Kotov, N.A., VanEpps, J.S., 2018. Unexpected insights into antibacterial activity of zinc oxide nanoparticles against methicillin resistant *Staphylococcus aureus* (MRSA). Nanoscale 10, 4927–4939. https://doi.org/10.1039/C7NR08499D.

Kirkwood, Z.I., Millar, B.C., Downey, D.G., Moore, J.E., 2018. Antimicrobial effect of dimethyl sulfoxide and N, N-Dimethylformamide on *Mycobacterium abscessus*: implications for antimicrobial susceptibility testing. Int. J. Mycobacteriol. 7, 134. https://doi.org/10.4103/ijmy.ijmy_35_18.

Klein, S., Kızaloğlu, M., Portilla, L., Park, H., Rejek, T., Hümmer, J., Meyer, K., Hock, R., Distel, L.V., Halik, M., 2018. Enhanced in vitro biocompatibility and water dispersibility of magnetite and cobalt ferrite nanoparticles employed as ROS formation enhancer in radiation cancer therapy. Small 14, 1704111. https://doi.org/10.1002/smll.201704111.

Kurimský, J., Rajňák, M., Bartko, P., Paulovičová, K., Cimbala, R., Medved', D., Džamová, M., Timko, M., Kopčanský, P., 2018. Experimental study of AC breakdown strength in ferrofluid during thermal aging. J. Mag. Mag. Mater. 465, 136–142. https://doi.org/10.1016/j.jmmm.2018.05.083.

Lei, W., Liu, Y., Si, X., Xu, J., Du, W., Yang, J., Zhou, T., Lin, J., 2017. Synthesis and magnetic properties of octahedral Fe_3O_4 via a one-pot hydrothermal route. Phys. Lett. A 381, 314–318. https://doi.org/10.1016/j.physleta.2016.09.018.

Li, Z., Ma, J., Ruan, J., Zhuang, X., 2019. Using positively charged magnetic nanoparticles to capture bacteria at ultralow concentration. Nanoscale Res. Lett. 14, 195. https://doi.org/10.1186/s11671-019-3005-z.

Liakos, I., Grumezescu, A.M., Holban, A.M., 2014. Magnetite Nanostructures as novel strategies for anti-infectious therapy. Molecules 19, 12710–12726. https://doi.org/10.3390/molecules190812710.

Maksoud, M.A., El-Sayyad, G.S., Ashour, A.H., El-Batal, A.I., Abd-Elmonem, M.S., Hendawy, H.A., Abdel-Khalek, E.K., Labib, S., Abdeltwab, E., El-Okr, M.M., 2018. Synthesis and characterization of metals-substituted cobalt ferrite $[M_xCo_{(1-x)}Fe_2O_4$;(M= Zn, Cu and Mn; x = 0 and 0.5)] nanoparticles as antimicrobial agents and sensors for *Anagrelide* determination in biological samples. Mater. Sci. Eng., C 92, 644–656. https://doi.org/10.1016/j.msec.2018.07.007.

Marinca, T.F., Chicinaş, H.F., Neamţu, B.V., Isnard, O., Pascuta, P., Lupu, N., Stoian, G., Chicinaş, I., 2016. Mechanosynthesis, structural, thermal and magnetic characteristics of oleic acid coated Fe_3O_4 nanoparticles. Mater. Chem. Phys. 171, 336–345. https://doi.org/10.1016/j.matchemphys.2016.01.025.

Mosafer, J., Abnous, K., Tafaghodi, M., Jafarzadeh, H., Ramezani, M., 2017. Preparation and characterization of uniform-sized PLGA nanospheres encapsulated with oleic acid-coated magnetic-Fe_3O_4 nanoparticles for simultaneous diagnostic and therapeutic applications. Colloids Surf. Physicochem. Eng. Asp. 514, 146–154. https://doi.org/10.1016/j.colsurfa.2016.11.056.

Mozaffari, S., Karimi, F., Sadat Khaloo, S., Barekat, A., 2015. Fabrication of a modified electrode based on multi-walled carbon nanotubes decorated with iron oxide nanoparticles for the determination of *Enrofloxacin*. Micro Nano Lett. 10, 561–566. https://doi.org/10.1049/mnl.2015.0123.

Navgare, D.L., Kawade, V.B., Tumberphale, U.B., Jadhav, S.S., Mane, R.S., Gore, S.K., 2020. Superparamagnetic cobalt-substituted copper zinc ferrialuminate: synthesis, morphological, magnetic and dielectric properties investigation. J. Sol-Gel Sci. Technol. 93, 633–642. https://doi.org/10.1007/s10971-019-05106-z.

Nehra, P., Chauhan, R., Garg, N., Verma, K., 2018. Antibacterial and antifungal activity of chitosan coated iron oxide nanoparticles. Br. J. Biomed. Sci. 75, 13–18. https://doi.org/10.1080/09674845.2017.1347362.

Oh, K.-I., Rajesh, K., Stanton, J.F., Baiz, C.R., 2017. Quantifying hydrogen-bond populations in dimethyl sulfoxide/water mixtures. Angew. Chem. Int. Ed. 56, 11375–11379. https://doi.org/10.1002/anie.201704162.

Purnama, B., Wijayanta, A.T., Suharyana,, 2019. Effect of calcination temperature on structural and magnetic properties in cobalt ferrite nano particles. J. King Saud Univ. – Sci. 31, 956–960. https://doi.org/10.1016/j.jksus.2018.07.019.

Raees, K., Ansari, M.S., Rafiquee, M.Z.A., 2020. Influence of surfactants and surfactant-coated IONs on the rate of alkaline hydrolysis of procaine in the presence of PEG. J. King Saud Univ. – Sci. 32, 1182–1189. https://doi.org/10.1016/j.jksus.2019.11.003.

Rezaei, N., Ehsani, M.H., Aghazadeh, M., Karimzadeh, I., 2018. An Investigation on magnetic-interacting Fe_3O_4 nanoparticles prepared by electrochemical synthesis method. J. Supercond. Novel Magn. 31, 2139–2147. https://doi.org/10.1007/s10948-017-4445-2.

Ruddaraju, L.K., Pammi, S.V.N., Guntuku, G Sankar, Padavala, V.S., Kolapalli, V.R.M., 2020. A review on anti-bacterials to combat resistance: from ancient era of plants and metals to present and future perspectives of green nano technological combinations. Asian J. Pharm. Sci. 15, 42–59. https://doi.org/10.1016/j.ajps.2019.03.002.

Saputro, R.E., Taufiq, A., Sunaryono, Hidayat, N., Hidayat, A., 2020. Effects of DMSO content on the optical properties, liquid stability, and antimicrobial activity of Fe_3O_4/OA/DMSO ferrofluids. NANO 15. https://doi.org/10.1142/S1793292020500678.

Saravanan, M., Gopinath, V., Chaurasia, M.K., Syed, A., Ameen, F., Purushothaman, N., 2018. Green synthesis of anisotropic zinc oxide nanoparticles with antibacterial and cytofriendly properties. Microb. Pathog. 115, 57–63. https://doi.org/10.1016/j.micpath.2017.12.039.

Shuai, J., Guan, F., He, B., Hu, Jianqing, Li, Y., He, D., Hu, Jianfeng, 2019. Self-assembled nanoparticles of symmetrical cationic peptide against *Citrus Pathogenic* bacteria. J. Agric. Food. Chem. 67, 5720–5727. https://doi.org/10.1021/acs.jafc.9b00820.

Sonohara, R., Muramatsu, N., Ohshima, H., Kondo, T., 1995. Difference in surface properties between *Escherichia coli* and *Staphylococcus* aureus as revealed by electrophoretic mobility measurements. Biophys. Chem. 55, 273–277. https://doi.org/10.1016/0301-4622(95)00004-h.

Stankic, S., Suman, S., Haque, F., Vidic, J., 2016. Pure and multi metal oxide nanoparticles: synthesis, antibacterial and cytotoxic properties. J. Nanobiotechnol. 14, 73. https://doi.org/10.1186/s12951-016-0225-6.

Sunaryono, Taufiq, A., Putra, E.G.R., Okazawa, A., Watanabe, I., Kojima, N., Rugmai, S., Soontaranon, S., Zainuri, M., Triwikantoro, 2016. Small-angle X-Ray scattering study on PVA/Fe_3O_4 magnetic hydrogels. Nano 11, 1650027. https://doi.org/10.1142/S1793292016500272.

Swatsitang, E., Phokha, S., Hunpratub, S., Usher, B., Bootchanont, A., Maensiri, S., Chindaprasirt, P., 2016. Characterization and magnetic properties of cobalt ferrite nanoparticles. J. Alloys Compd. 664, 792–797. https://doi.org/10.1016/j.jallcom.2015.12.230.

Taufiq, A., Saputro, R.E., Hidayat, N., Hidayat, A., Mufti, N., Diantoro, M., Patriati, A., Putra, E.G.R., Nur, H., 2017. Fabrication of magnetite nanoparticles dispersed in olive oil and their structural and magnetic investigations. In: IOP Conference Series: Materials Science and Engineering. IOP Publishing. https://doi.org/10.1088/1757-899X/202/1/012008.

Taufiq, A., Saputro, R.E., Hariyanto, Y.A., Hidayat, N., Hidayat, A., Mufti, N., Susanto, H., 2018. Functional group and magnetic properties of Fe_3O_4 ferrofluids: the impact of dispersion agent composition 012010. In: Journal of Physics: Conference Series. IOP Publishing. https://doi.org/10.1088/1742-6596/1093/1/012010.

Taufiq, A., Ikasari, F.N., Hidayat, N., Ulya, H.N., Saputro, R.E., Mufti, N., Hidayat, A., Sunaryono, S., Chuenchom, L., 2020. Dependence of PEO content in the preparation of Fe_3O_4/PEO/TMAH ferrofluids and their antibacterial activity. J. Polym. Res. 27, 1–10. https://doi.org/10.1007/s10965-020-02100-w.

Tena, N., Aparicio, R., García-González, D.L., 2017. Virgin olive oil stability study by mesh cell-FTIR spectroscopy. Talanta 167, 453–461. https://doi.org/10.1016/j.talanta.2017.02.042.

Thakur, D., Ta, Q.T.H., Noh, J.-S., 2019. Photon-induced superior antibacterial activity of palladium-decorated, magnetically separable Fe_3O_4/Pd/mpg-C_3N_4 nanocomposites. Molecules 24, 3888. https://doi.org/10.3390/molecules24213888.

Xiong, P., Yang, F., Ding, Z., Jia, Y., Liu, J., Yan, X., Chen, X., Yang, C., 2020. Preparation and electrocatalytic properties of spinel $Co_xFe_{3-x}O_4$ nanoparticles. Int. J. Hydrogen Energy 45, 13841–13847. https://doi.org/10.1016/j.ijhydene.2020.03.098.

Yang, B., Zhang, Q., Ma, X., Kang, J., Shi, J., Tang, B., 2016. Preparation of a magnetically recoverable nanocatalyst via cobalt-doped Fe_3O_4 nanoparticles and its application in the hydrogenation of nitroarenes. Nano Res. 9, 1879–1890. https://doi.org/10.1007/s12274-016-1080-3.

Yoon, B.K., Jackman, J.A., Valle-González, E.R., Cho, N.-J., 2018. Antibacterial free fatty acids and monoglycerides: biological activities, experimental testing, and therapeutic applications. Int. J. Mol. Sci. 19, 1114. https://doi.org/10.3390/ijms19041114.

Zafar, S., Ashraf, A., Ijaz, M.U., Muzammil, S., Siddique, M.H., Afzal, S., Andleeb, R., Al-Ghanim, K.A., Al-Misned, F., Ahmed, Z., Mahboob, S., 2020. Eco-friendly synthesis of antibacterial zinc nanoparticles using *Sesamum indicum L.* extract. J. King Saud Univ. – Sci. 32, 1116–1122. https://doi.org/10.1016/j.jksus.2019.10.017.

Zhang, Y., Cheng, X., Jiang, X., Urban, J.J., Lau, C.H., Liu, S., Shao, L., 2020a. Robust natural nanocomposites realizing unprecedented ultrafast precise molecular separations. Mater. Today 36, 40–47. https://doi.org/10.1016/j.mattod.2020.02.002.

Zhang, Y., Ma, J., Shao, L., 2020b. Ultra-thin trinity coating enabled by competitive reactions for unparalleled molecular separation. J. Mater. Chem. A 8, 5078–5085. https://doi.org/10.1039/C9TA12670H.